Spectroscopy and Regge trajectories of heavy quarkonia in the relativistic quark model

D. Ebert[a], R. N. Faustov[b], V. O. Galkin[b]

[a] *Institut für Physik, Humboldt–Universität zu Berlin,*
Newtonstr. 15, D-12489 Berlin, Germany
[b] *Dorodnicyn Computing Centre, Russian Academy of Sciences,*
Vavilov Str. 40, 119991 Moscow, Russia

Abstract

The mass spectra of charmonia and bottomonia are calculated in the framework of the relativistic quark model up to high orbital and radial excitations. The Regge trajectories of heavy quarkonia are constructed both in the (J, M^2) and (n_r, M^2) planes, where J is the total angular momentum and n_r is the radial quantum number. All daughter trajectories turn out to be almost linear and parallel, while parent trajectories exhibit some nonlinearity. Such nonlinearity occurs only in the vicinity of ground states and few lowest excitations and is more pronounced for bottomonia, while it is only marginal for charmonia. The obtained results are compared with available experimental data, and a possible interpretation of the new charmonium-like states above open charm production threshold is discussed.

1   Introduction

At present a vast amount of experimental data on the heavy quarkonium spectroscopy has been accumulated [1]. The number of known states is constantly increasing. Thus, in the last eight years more than ten new charmonium-like states have been discovered [2]. The total number of charmonium states, listed in the Particle Data Group Listings [1], is 25 at present. Some of the new states (such as $\eta_c(2S)$, h_c, $\chi_{c2}(2P)$, etc.) are the long-awaited ones, expected by quark models many years ago, while some others, with masses higher than the threshold of the open charm production, have narrow widths and unexpected decay properties [2]. There are theoretical indications that some of these new states could be the first manifestation of the existence of exotic hadrons (tetraquarks, molecules, hybrids etc.), which are expected to exist in QCD [3]. In order to explore such options, a comprehensive understanding of the heavy quarkonium spectroscopy up to rather high orbital and radial excitations is required. The LHCb Collaboration at the Large Hadron Collider (LHC) plans to search for the bottom counterparts of the newly discovered charmonium-like states [4]. At present, the experimentally known bottomonium spectrum consists of 20 states [1]. Therefore, the investigation of the masses of the excited heavy quarkonia states represents an important and interesting problem. To achieve this goal one should treat the quark dynamics in mesons completely relativistically. Here we extend the approach previously used for the investigations of light meson spectroscopy [5] to heavy quarkonia. In order to improve our description, leading radiative corrections to the heavy quark potential [6] are also taken into account. Such corrections are suppressed by additional powers of α_s, which are rather small for heavy quarkonia, and are known only in the framework of the v^2/c^2 expansion. Therefore we treat them perturbatively. The calculation of the masses of highly orbitally and radially excited states up to the fifths excitation is carried out. On this basis, the Regge trajectories for charmonia and bottomonia can be constructed both in the total angular momentum J and radial quantum number n_r, and properties like linearity, parallelism and equidistance of these trajectories can be checked . There are reasons to expect

that the parent Regge trajectories can be nonlinear [7, 8] due to the compactness of their ground and lowest excited states, which puts them in the region where both the linear confining and Coulomb parts of the quark-antiquark potential play an equally important role.

2 Relativistic quark model

In the relativistic quark model based on the quasipotential approach a meson is described by the wave function of the bound quark-antiquark state, which satisfies the quasipotential equation of the Schrödinger type [9]

$$\left(\frac{b^2(M)}{2\mu_R} - \frac{\mathbf{p}^2}{2\mu_R}\right)\Psi_M(\mathbf{p}) = \int \frac{d^3q}{(2\pi)^3}V(\mathbf{p}, \mathbf{q}; M)\Psi_M(\mathbf{q}), \tag{1}$$

where the relativistic reduced mass is

$$\mu_R = \frac{E_1 E_2}{E_1 + E_2} = \frac{M^4 - (m_1^2 - m_2^2)^2}{4M^3}, \qquad \text{with} \qquad E_{1,2} = \frac{M^2 - m_{2,1}^2 + m_{1,2}^2}{2M}. \tag{2}$$

Here $M = E_1 + E_2$ is the meson mass, $m_{1,2}$ are the quark masses, and $\mathbf{p}$ is their relative momentum. In the center-of-mass system the relative momentum squared on mass shell reads

$$b^2(M) = \frac{[M^2 - (m_1 + m_2)^2][M^2 - (m_1 - m_2)^2]}{4M^2}. \tag{3}$$

The kernel $V(\mathbf{p}, \mathbf{q}; M)$ in Eq. (1) is the QCD-motivated quasipotential operator of the quark-antiquark interaction, which is constructed with the help of the off-mass-shell scattering amplitude, projected onto the positive energy states. It is assumed that the effective interaction is the sum of the usual one-gluon exchange term with the mixture of long-range vector and scalar linear confining potentials

$$V(\mathbf{p}, \mathbf{q}; M) = \bar{u}_1(p)\bar{u}_2(-p)\left\{\frac{4}{3}\alpha_s D_{\mu\nu}(\mathbf{k})\gamma_1^\mu\gamma_2^\nu + V_{\text{conf}}^V(\mathbf{k})\Gamma_1^\mu\Gamma_{2;\mu} + V_{\text{conf}}^S(\mathbf{k})\right\}u_1(q)u_2(-q), \tag{4}$$

where the vector confining potential contains the Pauli interaction:

$$\Gamma_\mu(\mathbf{k}) = \gamma_\mu + \frac{i\kappa}{2m}\sigma_{\mu\nu}k^\nu. \tag{5}$$

Here α_s is the QCD coupling constant, $D_{\mu\nu}$ is the gluon propagator in the Coulomb gauge, γ_μ and $u(p)$ are the Dirac matrices and spinors and $\mathbf{k} = \mathbf{p} - \mathbf{q}$; κ is the Pauli interaction constant characterizing the anomalous chromomagnetic moment of quarks. Vector and scalar confining potentials in the nonrelativistic limit reduce to

$$V_{\text{conf}}^V(r) = (1 - \varepsilon)(Ar + B), \qquad V_{\text{conf}}^S(r) = \varepsilon(Ar + B), \tag{6}$$

where ε is the mixing coefficient. Therefore, in this limit the Cornell-type potential is reproduced

$$V_{\text{NR}}(r) = -\frac{4}{3}\frac{\alpha_s}{r} + Ar + B. \tag{7}$$

All the model parameters have the same values as in our previous papers [9, 5, 10]: the constituent quark masses $m_u = m_d = 0.33$ GeV, $m_s = 0.5$ GeV, $m_c = 1.55$ GeV, $m_b = 4.88$ GeV, and the parameters of the linear potential $A = 0.18$ GeV^2 and $B = -0.16$ GeV. The value of the mixing coefficient of vector and scalar confining potentials $\varepsilon = -1$ has been determined from the consideration of charmonium radiative decays [9] and matching heavy quark effective theory (HQET). Finally, the universal Pauli interaction constant $\kappa = -1$ has been fixed from the analysis of the fine splitting of heavy quarkonia ^3P_J- states [9]. In this case, the long-range

chromagnetic interaction of quarks, which is proportional to $(1+\kappa)$, vanishes in accordance with the flux-tube model.

The investigations of the heavy quark dynamics in heavy mesons indicate that the charm quark is not heavy enough to be considered as nonrelativistic. Indeed, estimates of the averaged velocity squared for the ground-state charmonium give the value $\langle v^2/c^2 \rangle \sim 0.25$. For excited charmonium states the $\langle v^2/c^2 \rangle$ values are even higher. Therefore, a reliable calculation of the charmonium spectroscopy requires a completely relativistic treatment of the charmed quark without an expansion in its velocity. The quasipotential (4) can in principal be used for arbitrary quark masses. The substitution of the Dirac spinors into (4) results in an extremely nonlocal potential in the configuration space. Clearly, it is very hard to deal with such potentials without any additional approximations. In order to simplify the relativistic $Q\bar{Q}$ potential, we make the following replacement in the Dirac spinors: $\epsilon_{1,2}(p) = \sqrt{m_{1,2}^2 + \mathbf{p}^2} \rightarrow E_{1,2}$ (see the discussion of this point in [5, 10]). This substitution makes the Fourier transformation of the potential (4) local. The resulting $Q\bar{Q}$ potential then reads

$$V(r) = V_{\mathrm{SI}}(r) + V_{\mathrm{SD}}(r), \tag{8}$$

where the explicit expression for the spin-independent $V_{\mathrm{SI}}(r)$ and spin-dependent $V_{\mathrm{SD}}(r)$ parts can be found in Ref. [5].

3   Results and discussion

3.1   Calculation of the mass spectra

We solve the quasipotential equation with the quasipotential (8), which nonperturbatively accounts for the relativistic dynamics of both heavy quarks, numerically. Then we add the one-loop radiative corrections and the additional one-loop correction for bottomonium due to the finite mass [9] of the charmed quark by using perturbation theory. The calculated masses of charmonia, bottomonia and the B_c meson are given in Tables 1,2, where $n = n_r + 1$, n_r is the radial quantum number, L, S and J are the quantum numbers of the orbital, total spin and total angular momenta, respectively. They are confronted with available experimental data from PDG [1], good agreement is found. It is important to note that the nonperturbative relativistic treatment gives a better agreement with data than our previous heavy quarkonium mass spectrum calculation [9], where only relativistic corrections up to v^2/c^2 order were taken into account. However, the differences between former and new predictions are rather small for most of the low-lying states and become noticeable only for higher excitations, where relativistic effects turn out to be particularly important.

3.2   Regge trajectories

In our analysis we calculated masses of both orbitally and radially excited heavy quarkonia up to rather high excitation numbers ($L = 5$ and $n_r = 5$). This makes it possible to construct the Regge trajectories in the (J, M^2) and (n_r, M^2) planes using the following definitions:
(a) the (J, M^2) Regge trajectory:

$$J = \alpha M^2 + \alpha_0; \tag{9}$$

(b) the (n_r, M^2) Regge trajectory:

$$n_r = \beta M^2 + \beta_0, \tag{10}$$

where α, β are the slopes and α_0, β_0 are the intercepts. The relations (9) and (10) arise in most models of quark confinement, but with different values of the slopes.

In Figs. 1-3 we plot the Regge trajectories in the (J, M^2) and (n_r, M^2) planes for charmonia and bottomonia. The fitted slopes and intercepts of the Regge trajectories are given in Tables 3

Table 1: Charmonium mass spectrum (in MeV).

State $n^{2S+1}L_J$	J^{PC}	Theory	Experiment meson	mass	State $n^{2S+1}L_J$	J^{PC}	Theory	Experiment meson	mass
1^1S_0	0^{-+}	2981	$\eta_c(1S)$	2980.3(1.2)	2^3D_1	1^{--}	4150	$\psi(4160)$	4153(3)
1^3S_1	1^{--}	3096	$J/\psi(1S)$	3096.916(11)	2^3D_2	2^{--}	4190		
2^1S_0	0^{-+}	3635	$\eta_c(2S)$	3637(4)	2^3D_3	3^{--}	4220		
2^3S_1	1^{--}	3685	$\psi(2S)$	3686.09(4)	2^1D_2	2^{-+}	4196	$X(4160)$?	$4156\binom{29}{25}$
3^1S_0	0^{-+}	3989			3^3D_1	1^{--}	4507		
3^3S_1	1^{--}	4039	$\psi(4040)$	4039(1)	3^3D_2	2^{--}	4544		
4^1S_0	0^{-+}	4401			3^3D_3	3^{--}	4574		
4^3S_1	1^{--}	4427	$\psi(4415)$	4421(4)	3^1D_2	2^{-+}	4549		
5^1S_0	0^{-+}	4811			4^3D_1	1^{--}	4857		
5^3S_1	1^{--}	4837			4^3D_2	2^{--}	4896		
6^1S_0	0^{-+}	5155			4^3D_3	3^{--}	4920		
6^3S_1	1^{--}	5167			4^1D_2	2^{-+}	4898		
1^3P_0	0^{++}	3413	$\chi_{c0}(1P)$	3414.75(31)	1^3F_2	2^{++}	4041		
1^3P_1	1^{++}	3511	$\chi_{c1}(1P)$	3510.66(7)	1^3F_3	3^{++}	4068		
1^3P_2	2^{++}	3555	$\chi_{c2}(1P)$	3556.20(9)	1^3F_4	4^{++}	4093		
1^1P_1	1^{+-}	3525	$h_c(1P)$	3525.41(16)	1^1F_3	3^{+-}	4071		
2^3P_0	0^{++}	3870			2^3F_2	2^{++}	4361		
2^3P_1	1^{++}	3906			2^3F_3	3^{++}	4400		
2^3P_2	2^{++}	3949	$\chi_{c2}(2P)$	3927.2(2.6)	2^3F_4	4^{++}	4434		
2^1P_1	1^{+-}	3926			2^1F_3	3^{+-}	4406		
3^3P_0	0^{++}	4301			1^3G_3	3^{--}	4321		
3^3P_1	1^{++}	4319			1^3G_4	4^{--}	4343		
3^3P_2	2^{++}	4354	$X(4350)$?	4351(5)	1^3G_5	5^{--}	4357		
3^1P_1	1^{+-}	4337			1^1G_4	4^{-+}	4345		
4^3P_0	0^{++}	4698			1^3H_4	4^{++}	4572		
4^3P_1	1^{++}	4728			1^3H_5	5^{++}	4592		
4^3P_2	2^{++}	4763			1^3H_6	6^{++}	4608		
4^1P_1	1^{+-}	4744			1^3H_5	5^{+-}	4594		
1^3D_1	1^{--}	3783	$\psi(3770)$	3772.92(35)					
1^3D_2	2^{--}	3795							
1^3D_3	3^{--}	3813	$X(3820)$	3823.5(2.5)					
1^1D_2	2^{-+}	3807							

and 4. We see that the calculated charmonium masses fit nicely to the linear trajectories in both planes (maybe with the exception of the parent trajectories, where the J/ψ and η_c mesons seem to have slightly lower masses). These trajectories are almost parallel and equidistant. For the bottomonium the situation is more complicated. The daughter trajectories, which involve both radially and orbitally excited states, turn out to be almost linear. On the other hand, the parent trajectories, which start from ground states, are exhibiting a nonlinear behaviour in the lower mass region. Such nonlinearity is most pronounced in bottomonium. The origin of this nonlinearity can be easily understood, if one compares the mean radii of these states. The values of the mean square radii $\sqrt{\langle r^2 \rangle}$ of charmonia and bottomonia, calculated in our model, are given in Table 5. The static potential of the quark-antiquark interaction is plotted in Fig. 4 (solid line). In this figure we also separately plot the contributions from linear confinement (dashed line) and of the modulus of the Coulomb potential (dotted line). As seen form Fig. 4, the Coulomb potential dominates for distances less than 0.15 fm, while the confining potential is dominant for distances larger than 0.5 fm. In the intermediate region both potentials play

Table 2: Bottomonium mass spectrum (in MeV).

State		Theory	Experiment		State		Theory
$n^{2S+1}L_J$	J^{PC}		meson	mass	$n^{2S+1}L_J$	J^{PC}	
1^1S_0	0^{-+}	9398	$\eta_b(1S)$	9390.9(2.8)	2^3D_1	1^{--}	10435
1^3S_1	1^{--}	9460	$\Upsilon(1S)$	9460.30(26)	2^3D_2	2^{--}	10443
2^1S_0	0^{-+}	9990	$\eta_b(2S)$	9974.6(3.2)	2^3D_3	3^{--}	10449
2^3S_1	1^{--}	10023	$\Upsilon(2S)$	10023.26(31)	2^1D_2	2^{-+}	10445
3^1S_0	0^{-+}	10329			3^3D_1	1^{--}	10704
3^3S_1	1^{--}	10355	$\Upsilon(3S)$	10355.2(5)	3^3D_2	2^{--}	10711
4^1S_0	0^{-+}	10573			3^3D_3	3^{--}	10717
4^3S_1	1^{--}	10586	$\Upsilon(4S)$	10579.4(1.2)	3^1D_2	2^{-+}	10713
5^1S_0	0^{-+}	10851			4^3D_1	1^{--}	10949
5^3S_1	1^{--}	10869	$\Upsilon(10860)$	10876(1)	4^3D_2	2^{--}	10957
6^1S_0	0^{-+}	11061			4^3D_3	3^{--}	10963
6^3S_1	1^{--}	11088	$\Upsilon(11020)$	11019(8)	4^1D_2	2^{-+}	10959
1^3P_0	0^{++}	9859	$\chi_{b0}(1P)$	9859.44(52)	1^3F_2	2^{++}	10343
1^3P_1	1^{++}	9892	$\chi_{b1}(1P)$	9892.78(40)	1^3F_3	3^{++}	10346
1^3P_2	2^{++}	9912	$\chi_{b2}(1P)$	9912.21(40)	1^3F_4	4^{++}	10349
1^1P_1	1^{+-}	9900	$h_b(1P)$	9898.25(1.50)	1^1F_3	3^{+-}	10347
2^3P_0	0^{++}	10233	$\chi_{b0}(2P)$	10232.5(6)	2^3F_2	2^{++}	10610
2^3P_1	1^{++}	10255	$\chi_{b1}(2P)$	10255.46(55)	2^3F_3	3^{++}	10614
2^3P_2	2^{++}	10268	$\chi_{b2}(2P)$	10268.65(55)	2^3F_4	4^{++}	10617
2^1P_1	1^{+-}	10260	$h_b(2P)$	10259.76(1.57)	2^1F_3	3^{+-}	10615
3^3P_0	0^{++}	10521			1^3G_3	3^{--}	10511
3^3P_1	1^{++}	10541	$\chi_b(3P)$	10530(11)	1^3G_4	4^{--}	10512
3^3P_2	2^{++}	10550			1^3G_5	5^{--}	10514
3^1P_1	1^{+-}	10544			1^1G_4	4^{-+}	10513
4^3P_0	0^{++}	10781			1^3H_4	4^{++}	10670
4^3P_1	1^{++}	10802			1^3H_5	5^{++}	10671
4^3P_2	2^{++}	10812			1^3H_6	6^{++}	10672
4^1P_1	1^{+-}	10804			1^3H_5	5^{+-}	10671
1^3D_1	1^{--}	10154					
1^3D_2	2^{--}	10161	$\Upsilon(1D)$	10163.7(1.4)			
1^3D_3	3^{--}	10166					
1^1D_2	2^{-+}	10163					

an equally important role. Therefore the light mesons and charmonia (with the exception of the η_c and J/ψ which are in the intermediate region) have characteristic sizes which belong to the region, where the confining potential dominates in the interquark potential (7). This leads to the emergence of the linear Regge trajectories. Contrary, the ground and few first excited states of bottomonia have smaller sizes and fall into the region, where the Coulomb part of the potential (7) gives an important contribution. As a result, the parent Regge trajectories of bottomonia are nonlinear, while the daughter trajectories (which fall into the region, where the confining potential is dominant) are still linear ones. In Ref. [7] an interpolating formula between the limiting cases of pure Coulomb and linear interactions was proposed. It can be written as follows:
(a) for the parent trajectory in the (J, M^2) plane

$$M^2 = \left(J - \frac{\gamma_1}{(J+2)^2} + \gamma_0 \right) / \gamma, \tag{11}$$
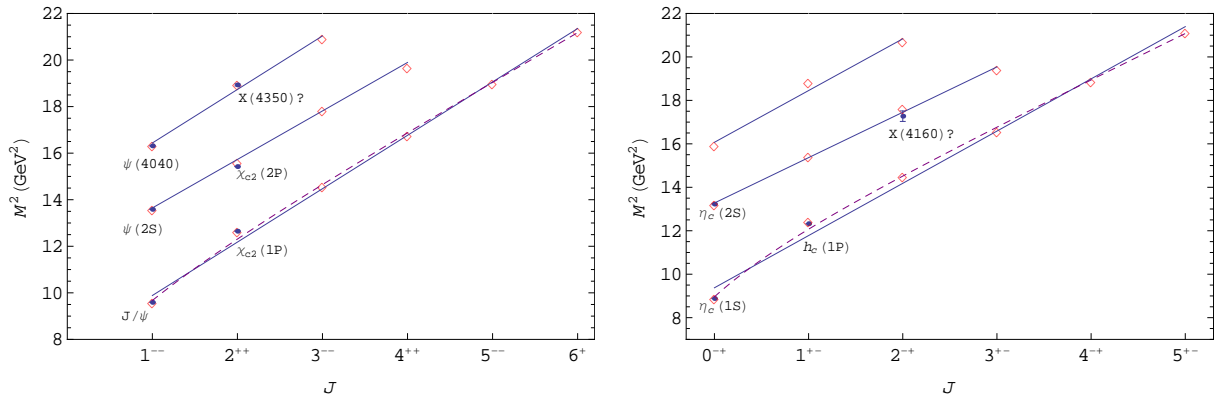
Figure 1: Parent and daughter (J, M^2) Regge trajectories for charmonium states with natural $(P = (-1)^J$, left) and unnatural parity $(P = (-1)^{J+1}$, right). Diamonds are predicted masses. Available experimental data are given by dots with particle names. The dashed line corresponds to a nonlinear fit for the parent trajectory.
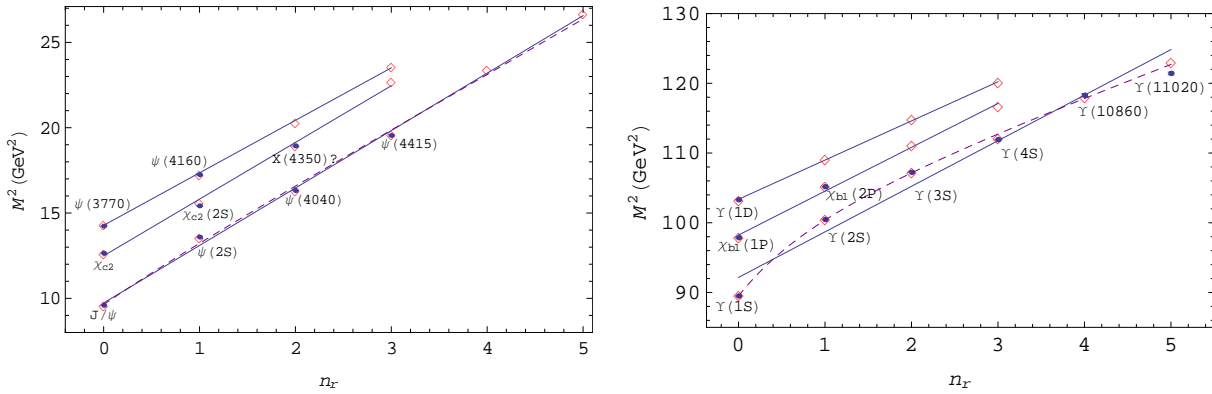

Figure 2: The (n_r, M^2) Regge trajectories for vector (S-wave), tensor and vector (D-wave) charmonium (left) and bottomonium (right) states (from bottom to top). Notations are the same as in Fig. 1.

(b) for the $J = 1$ trajectory in the (n_r, M^2) plane

$$M^2 = \left(n_r - \frac{\tau_1}{(n_r + 2)^2} + \tau_0 \right) / \tau, \tag{12}$$

where the parameters $\gamma, \tau, \gamma_0, \tau_0$ and γ_1, τ_1 determine the slopes, intercepts and nonlinearity of the Regge trajectories, respectively. Their fitted values are given in Table 6. The corresponding Regge trajectories are plotted in Figs. 1-3 by dashed lines. We see that the nonlinearity of the charmonium Regge trajectories is almost negligible, and its account does not significantly improve the quality of the fit compared to the linear one.

We can compare the slopes of linear Regge trajectories for heavy quarkonia obtained in this paper with our previous results for the slopes of Regge trajectories of light [5] and heavy-light [10] mesons. Such comparison shows that the slopes decrease rather fast with the growth of the quark masses: the slope α decreases from about 1.1 GeV^{-2} for light mesons, composed from u, d quarks and antiquarks, to about 0.24 GeV^{-2} for bottomonium. However, the difference between slopes of heavy-light $(Q\bar{q})$ mesons and of heavy quarkonia $(Q\bar{Q}')$ is not so dramatic. In fact, comparing the present Tables 3, 4 and the corresponding Tables 4, 5 of Ref. [10], we see that the slopes for charmonia and D, D_s mesons have very close values, and the same is true also for bottomonia, B_c and B, B_s mesons. This might indicate that the slope of the meson
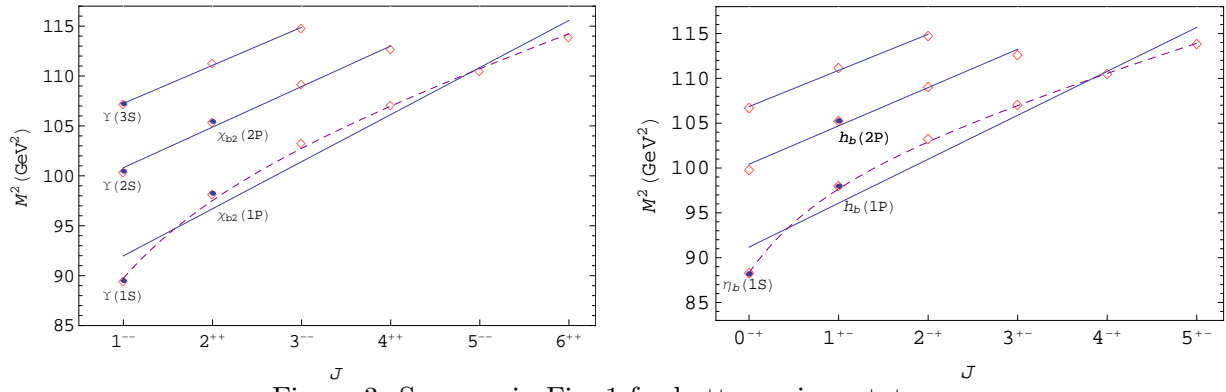
Figure 3: Same as in Fig. 1 for bottomonium states.

Table 3: Fitted parameters of the (J, M^2) parent and daughter Regge trajectories for heavy quarkonia.

Trajectory	natural parity		unnatural parity	
	α (GeV^{-2})	α_0	α (GeV^{-2})	α_0
$c\bar{c}$	J/ψ		η_c	
parent	0.436 ± 0.014	-3.31 ± 0.22	0.416 ± 0.021	-3.90 ± 0.31
first daughter	0.488 ± 0.011	-5.63 ± 0.18	0.479 ± 0.015	-6.36 ± 0.24
second daughter	0.431 ± 0.036	-6.08 ± 0.68	0.414 ± 0.050	-6.66 ± 0.92
$c\bar{c}$	χ_{c0}		χ_{c1}	
parent	0.431 ± 0.016	-5.07 ± 0.25	0.461 ± 0.008	-4.66 ± 0.12
daughter	0.493 ± 0.031	-7.41 ± 0.53	0.456 ± 0.006	-5.83 ± 0.11
$b\bar{b}$	Υ		η_b	
parent	0.212 ± 0.022	-18.5 ± 2.3	0.184 ± 0.024	-16.7 ± 2.5
first daughter	0.246 ± 0.014	-23.8 ± 1.5	0.234 ± 0.016	-23.5 ± 1.7
second daughter	0.262 ± 0.010	-27.1 ± 1.1	0.248 ± 0.014	-26.5 ± 1.6
$b\bar{b}$	χ_{b0}		χ_{b1}	
parent	0.228 ± 0.021	-22.3 ± 2.2	0.239 ± 0.018	-22.5 ± 1.9
daughter	0.254 ± 0.009	-26.7 ± 1.0	0.267 ± 0.006	-27.1 ± 0.7

Regge trajectory is mainly determined by the mass of the heaviest quark m_Q. The dependence of the Regge slopes α and β on m_Q has in both planes with rather good accuracy the same simple form: $\alpha, \beta \propto 1/\sqrt{m_Q}$.

3.3 Comparison with experiment

We first discuss the recently found quarkonium states below the open flavour production threshold. The observation and measurement of the mass of the pseudoscalar ground state η_b [1] provides a significant information about the spin-spin interaction in heavy quarkonia. The averaged bottomonium hyperfine splitting measured in $\Upsilon(3S) \to \eta_b(1S)\gamma$, $\Upsilon(2S) \to \eta_b(1S)\gamma$ and $\Upsilon(2S) \to \eta_b(2S)\gamma$ decays is $\Delta M_{\text{hfs}}(1S) \equiv M_{\Upsilon(1S)} - M_{\eta_b(1S)} = 69.3 \pm 2.8$ MeV and $\Delta M_{\text{hfs}}(2S) \equiv M_{\Upsilon(2S)} - M_{\eta_b(2S)} = 48.7 \pm 2.3 \pm 2.1$ MeV [1, 11]. Very recently the Belle Collaboration [12] reported the first observation of the radiative transitions $h_b(1P) \to \eta_b(1S)\gamma$ and $h_b(2P) \to \eta_b(2S)\gamma$. The measured $\eta_b(1S)$ mass is $9401.0 \pm 1.9^{+1.4}_{-2.4}$ MeV, $\eta_b(2S)$ mass is $9999.0 \pm 3.5^{+2.8}_{-1.9}$ MeV and the hyperfine splittings $\Delta M_{\text{hfs}}(1S) = 59.3 \pm 1.9^{+2.4}_{-1.4}$ MeV and $\Delta M_{\text{hfs}}(2S) = 24.3^{+4.0}_{-4.5}$ MeV [12]. Our predictions for these splittings, $\Delta M_{\text{hfs}}(1S) = 62$ MeV and $\Delta M_{\text{hfs}}(2S) = 33$ MeV, are in good agreement with the experimental values. Note that our model correctly predicts the branching ratios of the corresponding radiative decays [9].

7

Table 4: Fitted parameters of the (n_r, M^2) Regge trajectories for heavy quarkonia.

Meson	β (GeV^{-2})	β_0	Meson	β (GeV^{-2})	β_0
$c\bar{c}$			$c\bar{c}$		
η_c	0.287 ± 0.011	-2.62 ± 0.18	J/ψ	0.297 ± 0.010	-2.89 ± 0.16
χ_{c2}	0.301 ± 0.011	-3.76 ± 0.019	h_c	0.298 ± 0.010	-3.68 ± 0.17
$\psi(^3D_1)$	0.325 ± 0.006	-4.62 ± 0.11	$\psi(^3D_2)$	0.315 ± 0.003	-4.53 ± 0.06
$b\bar{b}$			$b\bar{b}$		
η_b	0.151 ± 0.013	-13.7 ± 1.4	Υ	0.153 ± 0.012	-14.1 ± 1.3
χ_{b2}	0.161 ± 0.007	-15.9 ± 0.7	h_b	0.161 ± 0.007	-15.8 ± 0.8
$\Upsilon(^3D_1)$	0.178 ± 0.002	-18.4 ± 0.3	$\Upsilon(^3D_2)$	0.178 ± 0.002	-18.4 ± 0.3

Table 5: Mean square radii $\sqrt{\langle r^2 \rangle}$ for the spin-singlet states of charmonia and bottomonia (in fm).

State	$\sqrt{\langle r^2 \rangle}_\psi$	$\sqrt{\langle r^2 \rangle}_\Upsilon$	State	$\sqrt{\langle r^2 \rangle}_\psi$	$\sqrt{\langle r^2 \rangle}_\Upsilon$
$1S$	0.37	0.22	$2D$	0.99	0.76
$1P$	0.59	0.41	$1H$	1.08	0.85
$2S$	0.71	0.50	$3P$	1.09	0.84
$1D$	0.74	0.54	$2F$	1.09	0.85
$2P$	0.87	0.65	$4S$	1.16	0.90
$1F$	0.87	0.65	$3D$	1.18	0.94
$3S$	0.94	0.72	$4P$	1.26	1.01
$1G$	0.98	0.75	$5S$	1.32	1.07

Another important experimental test of the structure of the spin splittings in heavy quarkonia comes from the measurement of the masses of the spin-singlet P levels first in charmonium $h_c(1P)$ [1] and very recently in bottomonium $h_b(1P)$ and $h_b(2P)$ [13]. The measured masses of these states almost coincide with the spin-averaged centroid of the triplet states $\langle M(^3P_J) \rangle = [M(\chi_{Q0}) + 3M(\chi_{Q1}) + 5M(\chi_{Q2})]/9$. The hyperfine mass splittings $\Delta M_{\rm hfs}(nP) \equiv \langle M(n^3P_J) \rangle - M(n^1P_1)$ in bottomonium are found to be $\Delta M_{\rm hfs}(1P) = (1.62 \pm 1.52)$ MeV and $\Delta M_{\rm hfs}(2P) = (0.48^{+1.57}_{-1.22})$ MeV [13]. This observation indicates that the spin-spin contribution is negligible for P levels, and thus shows the vanishing of the long-range chromomagnetic interaction in heavy quarkonia. In our model this is the result of the choice of the value of the long-range chromomagnetic quark moment $\kappa = -1$. Note that our original predictions [9] for
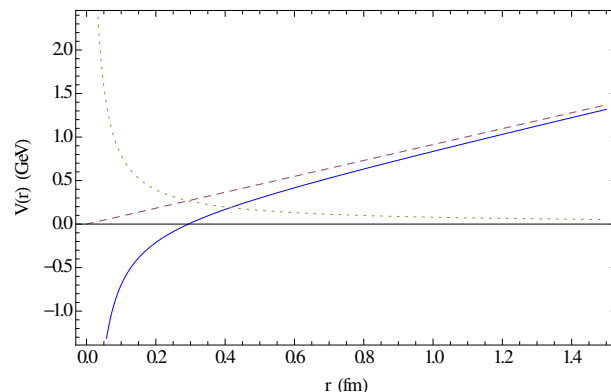

Figure 4: Static potential of the quark-antiquark interaction without the constant term (solid line). Dashed line shows the linear confining potential contribution, while dotted line corresponds to the modulus of the Coulomb potential.

Table 6: Fitted parameters of the nonlinear Regge trajectories for heavy quarkonia.

Meson	γ (GeV^{-2})	γ_0	γ_1	τ (GeV^{-2})	τ_0	τ_1
Υ	0.33	32.2	32.3	0.22	22.2	10.1
η_b	0.33	32.9	15.0			
χ_{b0}	0.33	33.7	6.57			
J/ψ	0.48	4.25	5.47	0.31	3.19	0.82
η_c	0.48	5.19	3.56			

the spin-singlet masses are confirmed by these measurements.

The recently observed $\Upsilon(1^3D_2)$ state is the only D-wave state found below the threshold of open flavour production. Our prediction for its mass (see Table 2) is in good agreement with the measured value. It will be interesting to observe other $\Upsilon(1D)$ states in order to test further our understanding of spin-orbit and spin-spin interactions in heavy quarkonia. The mass of the newly observed $\chi_b(3P)$ state is also in accord with our prediction.

Next we discuss the observed states above the open flavour production threshold. The most well-established states are the vector 1^{--} states. For charmonium PDG [1] lists seven such states: $\psi(3770)$, $\psi(4040)$, $\psi(4160)$, $X(4260)$, $X(4360)$, $\psi(4415)$ and $X(4660)$, from which only the ψ states are included in the PDG Summary Tables [1]. These states are believed to be ordinary $c\bar{c}$ charmonium (with isospin $I = 0$). They are well described by our model (see Table 1): $\psi(4040)$ and $\psi(4415)$ are the 3^3S_1 and 4^3S_1 states, while $\psi(3770)$ and $\psi(4160)$ are the 1^3D_1 and 2^3D_1 states, respectively. These ψ states fit well to the corresponding Regge trajectories (see Fig. 2). On the other hand, the three new vector states X are considered as unexpected exotic states (their isospin is not determined experimentally). Indeed, we do not have any $c\bar{c}$ candidates for these states in Table 1. Contrary, in Ref. [14] we have found that these states can be described in our model as tetraquarks composed from a diquark and antidiquark ($[cq][\bar{c}\bar{q}]$, $q = u, d$). In particular, the $X(4260)$ and $X(4660)$ states can be interpreted as the 1^{--} states of such tetraquarks with a scalar diquark $[cq]_{S=0}$ and scalar antidiquark $[\bar{c}\bar{q}]_{S=0}$ in the relative $1P$ and $2P$ states and predicted masses 4244 MeV and 4666 MeV, respectively [14]. The $X(4360)$ can be viewed as the 1^{--} tetraquark with the axial vector diquark $[cq]_{S=1}$ and axial vector antidiquark $[\bar{c}\bar{q}]_{S=1}$ in the relative $1P$ state, which mass is predicted to be 4350 MeV [14].

The three vector bottomonium states, $\Upsilon(10580)$, $\Upsilon(10860)$ and $\Upsilon(11020)$, observed above open bottom threshold [1], are rather well described in our model as 4^3S_1, 5^3S_1 and 6^3S_1 states (see Table 2), the mass of $\Upsilon(11020)$ being somewhat higher than the experimental value. They fit to the corresponding Regge trajectory in Fig. 2.

The only experimentally established $2P$ charmonium state is $\chi_{c2}(2P)$ which mass is predicted slightly higher (by about 20 MeV) in our model. From Table 1 we see that the exotic state $X(3872)$ cannot be described as the 1^{++} 2^3P_1 $c\bar{c}$ state or the 2^{-+} 1^1D_2 $c\bar{c}$ state. If this state belonged to either $2P$ or $1D$ multiplets, this could signal a large fine splitting in these multiplets, since the $X(3872)$ mass is 55 MeV below $\chi_{c2}(2P)$ and 100 MeV above $\psi(3770)$. As we see from Table 1, our model does not support such large fine splittings. In Ref. [14] we argued that $X(3872)$ can be considered as the 1^{++} ground state tetraquark, composed from the scalar and axial vector diquark and antidiquark $(([cq]_{S=0}[\bar{c}\bar{q}]_{S=1} + [cq]_{S=1}[\bar{c}\bar{q}]_{S=0})/\sqrt{2})$, which mass is predicted to be 3871 MeV.

As we see from Table 1, the $X(4160)$ and $X(4350)$ can be attributed from the point of view of the mass value and charge parity $C = +$ to the pseudo tensor 2^{-+} spin-singlet 2^1D_2 and tensor 2^{++} spin-triplet 3^3P_2 charmonium states, respectively. They fit well to the corresponding Regge trajectories in Figs. 1-2.

The $X(4140)$ state, observed by CDF in $B^+ \to K^+\phi J/\psi$ decays [15], can correspond in our model to the scalar 0^{++} charmed-strange diquark-antidiquark $[cs]_{S=1}[\bar{c}\bar{s}]_{S=1}$ ground state,

which predicted mass is 4110 MeV, or the axial vector 1^{++} one $([cs]_{S=0}[\bar{c}\bar{s}]_{S=1}+[cs]_{S=1}[\bar{c}\bar{s}]_{S=0})/\sqrt{2}$) with calculated mass 4113 MeV [14].

Two of the three charmonium-like charged $X^{\pm}$ states reported by Belle [16], which are explicitly exotic, can be interpreted in our model as tetraquark states. We do not have tetraquark candidate for the $X(4040)^{+}$ structure, while the $X(4250)^{+}$ can be considered as the charged partner of the 1^{-} $1P$ state $[cu]_{S=0}[\bar{c}\bar{d}]_{S=0}$ or as the 0^{-} $1P$ state of the $([cu]_{S=0}[\bar{c}\bar{d}]_{S=1} + [cu]_{S=1}[\bar{c}\bar{d}]_{S=0})/\sqrt{2}$) tetraquark with predicted masses 4244 MeV and 4267 MeV, respectively [14]. The $X(4430)^{+}$ could be the first radial $(2S)$ excitation of the 1^{+} $X(3872)$ tetraquark or the 0^{+} $2S$ $[cu]_{S=1}[\bar{c}\bar{d}]_{S=1}$ tetraquark, which have very close masses 4431 MeV and 4434 MeV [14].

As we see, a consistent picture of the excited quarkonium states emerges in our model. All well-established states and most of the states, which need additional experimental confirmation, can be interpreted as excited quarkonium or diquark-antidiquark tetraquark states.

4 Conclusions

The mass spectra of charmonia, bottomonia and B_c mesons were calculated in the framework of the relativistic quark model based on the quasipotential approach. Highly radially and orbitally excited quarkonium states were considered. On this basis, the Regge trajectories of heavy quarkonia were constructed both in the (J, M^2) and (n_r, M^2) planes. A different behaviour of these trajectories was observed for parent and daughter trajectories. All daughter trajectories turn out to be almost linear and parallel, while parent trajectories exhibit some nonlinearity. Such nonlinearity occurs only in the vicinity of ground states and few lowest excitations and is mostly pronounced for bottomonia. For charmonia this nonlinearity is only marginal, and its account does not significantly improve the fit. It was shown that the masses of the excited states of heavy quarkonia are determined by the average distances between quarks larger than 0.5 fm, where the linear confining part of the quark-antiquark interaction dominates. This leads to the emergence of almost linear Regge trajectories. On the other hand, a few lowest quarkonium states have average sizes smaller than 0.5 fm and fall in the region, where both the Coulomb and confining potentials play an important role. As a result, the parent Regge trajectories exhibit a certain nonlinearity in this region. The parameters (slopes, intercepts and nonlinearity) of both linear and nonlinear Regge trajectories were determined. They were compared to the slopes of the linear Regge trajectories of light [5] and heavy-light [10] mesons calculated previously. It was found that the slope of the meson Regge trajectory is mainly determined by the mass of the heaviest quark m_Q.

A detailed comparison of the calculated heavy quarkonium masses with available experimental data was carried out. It was found that all data for the states below open flavour production threshold are well reproduced in our model: the difference between predicted and measured masses does not exceed few MeV. For higher excited states, which are above this threshold, most of the well-established conventional states are also well described by our approach, the difference between theory and experiment being somewhat larger, but still within 20 MeV. In this case the multichannel consideration is desirable. It was shown that these states fit well to the corresponding Regge trajectories. Other states, which have unexpected properties and are therefore believed to have an exotic origin, were also discussed. As it was shown in our previous calculation [14], most of these states can be described as diquark-antidiquark tetraquarks. Therefore we have a self-consistent picture of the heavy quarkonium spectra. Future experimental studies of yet unobserved conventional quarkonium states and a clarification of the nature and quantum numbers of the exotic quarkonium-like states will provide an additional test of our model.

References

[1] J. Beringer et al. [Particle Data Group], "Review of Particle Physics," Phys. Rev. D **86**, 010001 (2012); J. Li, arXiv:1209.4392 [hep-ex].

[2] N. Brambilla *et al.*, Eur. Phys. J. C **71**, 1534 (2011).

[3] E. Klempt and A. Zaitsev, Phys. Rept. **454**, 1 (2007).

[4] L. L. Gioi, arXiv:1109.3398 [hep-ex].

[5] D. Ebert, R. N. Faustov and V. O. Galkin, Phys. Rev. D **79**, 114029 (2009).

[6] S. Gupta and S. F. Radford, Phys. Rev. D **24**, 2309 (1981); ibid. **25**, 3430 (1982); J. Pantaleone, S.-H. H. Tye and Y. J. Ng, Phys. Rev. D **33**, 777 (1986).

[7] M. N. Sergeenko, Z. Phys. C **64**, 315 (1994); S. S. Gershtein, A. K. Likhoded and A. V. Luchinsky, Phys. Rev. D **74**, 016002 (2006).

[8] A. M. Badalian, Phys. Atom. Nucl. **74**, 1375 (2011).

[9] D. Ebert, R.N. Faustov and V.O. Galkin, Phys. Rev. D **67**, 014027 (2003).

[10] D. Ebert, R. N. Faustov and V. O. Galkin, Eur. Phys. J. C **66**, 197 (2010).

[11] S. Dobbs, Z. Metreveli, K. K. Seth, A. Tomaradze and T. Xiao, Phys. Rev. Lett. **109**, 082001 (2012).

[12] I. Adachi *et al.* [Belle Collaboration], arXiv:1110.3934 [hep-ex]; R. Mizuk *et al.* [Belle Collaboration], arXiv:1205.6351 [hep-ex].

[13] J. P. Lees [The BABAR Collaboration], arXiv:1102.4565 [hep-ex]; I. Adachi *et al.* [Belle Collaboration], arXiv:1103.3419 [hep-ex].

[14] D. Ebert, R. N. Faustov and V. O. Galkin, Phys. Lett. B **634**, 214 (2006); Eur. Phys. J. C **58**, 399 (2008); Mod. Phys. Lett. A **24**, 567 (2009).

[15] T. Aaltonen *et al.* [CDF Collaboration], Phys. Rev. Lett. **102**, 242002 (2009).

[16] S. K. Choi *et al.* [Belle Collaboration], Phys. Rev. Lett. **100**, 142001 (2008); R. Mizuk *et al.* [Belle Collaboration], Phys. Rev. D **78**, 072004 (2008); Phys. Rev. D **80**, 031104 (2009).